ELABORAREA ŞI CARACTERIZAREA UNOR NOI BIOCOMPOZITE RANFORSATE CU FIBRE DE STICLĂ DESTINATE RECONSTRUCŢIEI OSOASE CRANIENE

DEVELOPMENT AND CHARACTERIZATION OF NEW FIBER-REINFORCED BIOCOMPOSITES FOR CRANIAL BONE RECONSTRUCTION

MĂDĂLINA-ANCA LAZĂR[1]* , MIUŢA FILIP[2], MIHAELA CECILIA VLASSA[2], LIDIA ADRIANA SORCOI[3], RADU SEPTIMIU CÂMPIAN[4], CRISTINA PREJMEREAN[2]

[1]*"Iuliu Haţieganu" University of Medicine and Pharmacy, Department of Implantology and Maxillofacial Surgery, 33 Moţilor Str, 40001 Cluj-Napoca, Romania*

[2]*"Babeş Bolyai" University, "Raluca Ripan" Institute for Research in Chemistry, 30 Fântânele Str, 400294 Cluj-Napoca, Romania*

[3]*Technical University, Department of Materials Science and Engineering, 103-105 Muncii Avenue, 400641Cluj-Napoca, Romania*

[4]*"Iuliu Haţieganu" University of Medicine and Pharmacy, Department of Oral Rehabilitation, 15 Babeş Str, 400012 Cluj-Napoca, Romania*

The aim of the present study was the elaboration and the characterization of new fiber-reinforced composites (FRCs) that will serve cranial bone reconstruction, particularly in the cases of large bicortical calvarial defects. A series of resins containing dimethacrylate and urethane-dimethacrylate monomers were prepared and characterized. The most promising resin was selected in order to be reinforced with continuous unidirectional and woven E-glass fibers, respectively. The elaborated FRCs were investigated in vitro by scanning electron microscopy (SEM) and by determining the flexural properties and in vivo by intramuscular implantation test. The results of this study pointed out that the FRCs based on urethane dimethacrylic resin reinforced with woven E-glass fibers could be good candidates for the reconstruction of large cranial bone defects.

Scopul studiului de faţă a fost elaborarea şi caracterizarea unor noi materiale compozite armate cu fibre de sticlă (FRC) destinate reconstrucţiei osoase craniene, în cazul defectelor de mari dimensiuni, bicorticale, ale calvariei. Au fost preparate şi caracterizate o serie de răşini pe bază de monomeri dimetacrilici şi uretan-dimetacrilici. Răşina cu cele mai bune proprietăţi a fost selectată în vederea ranforsării cu fibre continue, unidirecţionale şi respectiv cu ţesătură de fibre de sticlă E. Materialele compozite elaborate au fost investigate in vitro prin microscopie electronică de baleiaj (SEM) şi prin determinarea rezistenţei la încovoiere şi in vivo prin teste de implantare intramusculară. Rezultatele studiului arată că materialele compozite pe bază de răşini uretan-dimetacrilice ranforsate cu ţesătură de fibre de sticlă E reprezintă o alegere optimă pentru reconstrucţia defectelor osoase craniene extinse.

Keywords: *biomaterials, bone reconstruction, fiber-reinforced composite, residual monomer, flexural strength, biocompatibility*

1. Introduction

In spite of the huge progress made in reconstructive surgery in recent decades, restoring cranio-facial bone structures remains an endless challenge. Materials and techniques used to serve this purpose were of great diversity, but so far, there is no optimal method for reconstruction of large cranial bone defects. Over time, metal plates, xenografts, allogenic or autologous bone grafts, ceramics and polymers have been used [1, 2].

For decades, the gold standard in bone reconstruction was considered the autologous bone graft [3, 4]. Unfortunately, the use of autologous grafts has drawbacks and risks related to the additional morbidity of the donor site, to the difficulty and even the impossibility to conform the bone graft to the shape and size of the receptor site. There are also additional risks of resorption of bone graft, as well as the risk of necrosis and/or infection [5, 6]. In this context, the use of biomaterials in bone reconstruction is the direction all research concerns in medicine and its related fields should embrace.

The need for patient-specific implants in solving complex cases of bone reconstruction is widely accepted as a real fact of modern medicine. The clinical use of customized implants, with their unique ability of restoring in detail the anatomy affected by congenital or acquired pathology, creates the premises to optimal functional restoration and has numerous advantages: significant increase in the quality of reconstruction, effective planning of surgery, reduced surgery time and recovery period, lasting therapeutic solution (without the risk of resorption or graft necrosis) [7-10]. In spite of all the improvements in the field of bone reconstruction, present day biomaterials still have some shortcomings that limit their application

* Autor corespondent/*Corresponding author*,
E-mail: madilazar@yahoo.com

and sometimes cause clinical problems [1, 11].

When metal is used for producing implants, it has the disadvantages of thermal conduction (which can cause problems to the patient), different mechanical properties from the bone (that impair healing due to "stress-shielding effect") and difficulty in intraoperative modeling of the implant when this is necessary. The artefacts produced by metals during imaging (CT, MRI) of the operated area are notable, making the diagnostic process difficult [12-14].

Calcium phosphate and calcium sulphate ceramics represent a group of materials with different handling, morphological, mechanical and degradation properties. Although extensively used in the past decades, calcium phosphate showed high, long-term complication rate and the material was contraindicated for large, full-thickness, skull defects by some authors [15, 16].

Bioactive glasses possess both osteointegrative and osteoconductive properties. When used as a preformed implant they have significantly greater mechanical strength when compared to calcium phosphate. However, bioactive glass blocks do not resist drilling and shaping and they may fracture during the process. As a consequence they are difficult to fix to the skeleton [17, 18].

Polymethylmethacrylate (PMMA) has brought new solutions in reconstructing large craniofacial defects by rapid prototyping modelling technologies (ex-vivo, in the preoperative phase). But, there is no bone incorporation or ingrowth, making it susceptible to infection throughout the reconstruction. If the patient had experienced a previous infection in the region of implantation, the risk of infection after PMMA cranioplasty is markedly increased [19].

Polyetheretherketone (PEEK) is an aromatic polymer with ether and ketone chains that may be a safe alternative in the reconstruction of the cranial vault. Among the advantages of the use of PEEK, less surgical time and the fact that there is no need for remodelling as it is sometimes necessary when using bone or methyl-methacrylate are mentioned. If it eventually has to be replaced, it can be sterilised and used again. Still, the material has some disadvantages, which are expensiveness, risk of postoperative infection, lack of bioactive potential [20, 21].

These shortcomings fuel the continual search for better implant materials.

The aim of the present study was the elaboration and characterization of new advanced biomaterials based on fiber-reinforced composites (FRCs) that will serve cranial bone reconstruction, in case of large bicortical calvarial defects.

2. Experimental

2.1. Materials

1,6-bis(methacryloxy-2-ethoxy-carbonyl-amino)-2,4,4-trimethyl-hexane (UDMA), triethylene glycol dimethacrylate (TEGDMA), 2-hydroxyethyl methacrylate (HEMA), benzoyl peroxide (POB), (N,N-dihydroxyethyl-p-toluidine (DHEPT), butylated hydroxy toluene (BHT) were purchased from Sigma Aldrich Chemical Co. (Taufkirchen, Germany) and used without additional purification. The Bis-GMA-type oligomers containing 93% monomer (2,2-bis[4-(2-hydroxy-3-methacryloxypropoxy) phenyl]propane and 7% dimmer were synthesized in our laboratory using the method described previously [22]. The E-glass fibers (300g/mp) were purchased from Owens Corning, Brussels, Belgium.

2.2. The preparation of the monomer mixtures (resins)

The experimental monomer mixtures are prepared using Bis-$GMA_{1,2}$ or UDMA as base monomers and TEGDMA or HEMA as diluting monomers. The ratio between the monomers is showed in Table 1:

Table 1

Resins used in the study/ *Răşinile utilizate în studiu*

Resin	Bis-$GMA_{1.2}$ %	UDMA %	TEGDMA %	HEMA %
Resin 1	60		40	
Resin 2	60			40
Resin 3	10	60	30	
Resin 4	10	60		30

2.3. The preparation of the copolymers by chemical initiation of polymerization

In order to obtain the copolymers by chemical initiation of polymerization, two monomer mixtures were prepared for each copolymer, which had the same monomer amount, as presented in table 1: a base resin and a catalyst resin. In the base resin was dissolved 2% by weight of the polymerization accelerator (N,N-dihydroxyethyl-p-toluidine, DHEPT) and in the catalyst resin was added 2% by weight of the polymerization initiator, benzoyl peroxide (POB). Butylated hydroxytoluene (BHT) was used as an inhibitor in an amount of 0.1% by weight. Disk copolymers of 5 mm diameter and 0.5 mm thickness were obtained by mixing equal amounts of base resins with

corresponding catalyst resins in a teflon mold. The initial polymerization took place under a polyethylene band in order to prevent the contact with the atmospheric oxygen. Then the copolymers were subjected to a post-curing treatment at 100^0C for 2 hours.

2.4. The preparation of the glass fiber-reinforced composites (FRC)

To ensure good interfacial adhesion and stress transfer across the interface, E glass fibers were treated with a coupling agent [23, 24]. 1 wt % A-174 (γ-methacryloxypropyl-1-trimethoxysilane) was added to the amount of E-glass fibers. The silane solution was prepared by dissolving A-174 silane in ethanol–water 90/10 vol.% acidified to pH 3.8. PH level was maintained using glacial acetic acid. The glass fibers were immersed in this solution for 1 h. After that, the silane layer was dried at 110 °C for 2 h [25].

Each FRC was obtained using the laminate lay-up process. The bottom layer in the mold was the base resin, over which the continuous unidirectional or bi-woven E- glass fibers treated with silane A-174 were applied. On the top surface of this last material a layer of catalyst resin was added. Then the glass fibers and the resins were applied alternatively using the following pattern: base resin, unidirectional /woven glass fibers, catalyst resin, unidirectional /woven glass fibers, base resin, etc. The FRCs hardened through the chemically initiated polymerization of the resins at room temperature. In order to avoid the presence of potential irritating fiber glass edges on the surface of the implants, the FRC hardened samples were covered with a final coating comprising a first layer made of the catalyst resin and a second layer made of the base resins, respectively. Then, the implants were submitted to thermic treatment (post-polymerization) for 2 hours at 100^0C in an oven. The polymerization started the moment a base resin was mixed with a catalyst resin and continued during the application of the successive layers of resins and E-glass fibers. Surface morphology of the samples was assessed by scanning electron microscopy (SEM).

2.5. Determination of the residual double bonds by FTIR spectroscopy

The conversion of monomer mixtures was evaluated by determining the residual double bonds using the Infrared Spectroscopy Method. The quantity of unreacted methacrylate groups was determined in percent of the methacrylate groups originally present in the unpolymerized material. The decrease in the intensity of the methacrylate C=C absorbance (Ameth) at 1635 -1640 cm^{-1} was monitored. The phenyl absorbance (Aarom) at 1605-1610 cm^{-1} was used as an internal standard [26]. The degree of conversion was calculated using the formulas:

$$RDB\% = (A_{meth}/A_{arom})_F / (A_{meth}/A_{arom})_I \; x100 \quad (1)$$

where F means the final state (after curing) and I means the initial state of the material (before curing).

$$DC\% = 100\%-RDB\% \quad (2)$$

ATR-FTIR spectra of liquid monomer mixtures (resins) and solid copolymers were recorded on FTIR spectrophotometer (Jasco FTIR-610) equipped with an ATR (attenuated total reflectance) attachment with a horizontal ZnSe crystal (Jasco PRO400S). The resolution of the spectra was 4 cm^{-1}, and scans were repeated 100 times. The appropriate amount of the samples was placed on the ZnSe crystal and then the FTIR spectrum was measured.

2.6. Determination of the residual monomers by HPLC

The cured FRC were weighted and extracted in 25 ml alcoholic solution (70% etilic alcohol, 30% water), 7 days at room temperature. The alcoholic extracts (25 mL) were rota-evaporated to dryness and resuspended at 2 mL of acetonitrile, filtered in 0.22 μm PTFE filters, and analyzed by HPLC. The linearity of the response to analytes was established with four concentration levels and the regression factors R^2 were >0.998.

The analyses were carried out on a HPLC Jasco Chromatograph (Japan) equipped with an HPLC pump (Model PU-980), a ternary gradient unit (Model LG-980-02), an column thermostat (Model CO-2060 Plus), an UV/VIS detector (Model UV-975) and an injection valve equipped with a 20μL sample loop (Rheodyne). The samples were injected manual with a Hamilton Rheodyne Syringe (50 mL). The system was controlled and the experimental data analyzed with the ChromPass software.

Separation was carried out on a Lichrosorb RP-C18 column (25 x 0.46 cm) at 21 ºC column temperature. The mobile phase was a mixture of acetonitrile (A, HPLC grade) and water (Milipore ultrapure water) and a gradient was applied according to the following method: 0-15 min. linear gradient 50–80% A; 15–25 min. linear gradient 80–50% A. The flow rate was 0.9 mL min^{-1} and the injector volume was always 20 mL. UV detection was performed at 204 nm for monitoring the elution of all analytes (BisGMA, TEGDMA, HEMA and UDMA) because they exhibit significant absorption at this wavelength. The compounds were identified by comparison of their elution times with those of the reference compounds under the same HPLC conditions.

2.7. Determination of flexural properties of the experimental FRCs

The *flexural strength and modulus of elasticity* were determined using FRC specimens having rectangular form (length 25.0 mm, height 2.0 mm and width 2.0 mm), according to ISO 4049/2000 three-point bending test. The measurements of the flexural properties were made using a Lloyd LR5K Plus mechanical testing apparatus connected with a computer. The crosshead speed of the testing machine was 1.0 mm/min.

2.8. Scanning electron microscopy (SEM)

To highlight some details about the appearance and structure of composites before and after the flexural test, the FRCs were examined by SEM (JEOL. JSM 5600 LV) equipped with EDX spectrometer (Oxford Instruments Soft Inca 200). The samples were coated with gold (25 A°) using the DESK V apparatus prior to analysis.

2.9. Biological assay

In order to assess the biological behaviour of the formulated FRC, samples of 3 mm long and 2 mm diameter were prepared and sterilized using plasma (Sterrad, J&J, Irvine, CA, USA). The animal study was carried out following the guidelines and protocols of the Ethics Committee of "Iuliu Haţieganu" University of Medicine and Pharmacy, Cluj-Napoca. Twenty male Wistar Rats, weighing about 250g each, were randomly divided in two groups of 10 animals, according to the FRC tested: cFRC (continuous unidirectional bundles of fiber glass and resin R3), wFRC (woven fiber glass and resin R3). The implants were surgically inserted into the thigh muscle.

After placing the samples, the experimental animals were put into identified cages and received a normal diet (solid food) and water *ad libitum* during the entire study period. During the experiment period, assessments were made regarding the local changes, which occurred at the implant site and their impact upon the general status of the animals. All animals were sacrificed 30 days after implantation, following the guidelines of the Ethics Committee. Tissues surrounding the implants were macroscopically analyzed. Implants were sharply removed together with the adjacent muscle. Tissue samples from the areas that contained the implants were prepared for histological analysis.

The tissue adjacent to the implant was evaluated and a descriptive analysis of the histological findings was made. The following features were assessed: number and type of inflammatory cells (polymorphonuclear cells, lymphocytes, plasma cells, macrophages and giant cells), aspect of the adjacent blood vessels and presence of necrosis, fibrosis and fatty infiltrate. Each criterion was evaluated according to ISO standards [27] and irritant ranking of the materials assessed accordingly.

3. Results and discussion

3.1. Residual double bonds

A cross-linked three-dimensional network is formed by the polymerization of the monomer mixtures existing in the di(meth)acrylic resins. During the polymerization of dimethacrylate monomers, the gel effect occurs, leading to the closing of radicals and unreacted monomers in the cross-linked network [28]. Presence of residual monomer or unreacted double bonds in the harden matrix has a plasticizing effect on the polymer. More than that, residual double bonds can make the polymeric matrix more susceptible to degradative reactions.

Table 2 shows the degree of conversion (%) of the investigated copolymers at 1 day after the initial polymerization of the appropriate resins.

Table 2

Degree of conversion obtained for the experimental copolymers/ *Gradele de conversie obţinute pentru copolimerii experimentali*

Copolymer samples	DC (%)			
	C1	C2	C3	C4
after 1 day	73.62	63.45	85.58	63.82

Table 3

Calculation of residual double bonds (RDB) for the experimental copolymers
Calculul dublelor legături reziduale pentru copolimerii experimentali

Sample	Abs_i 1635.34 cm^{-1}	Abs_i 1606.41 cm^{-1}	Abs_f 1637.27 cm^{-1}	Abs_f 1608.34 cm^{-1}	r_i	r_f	RDB %
FRC1	0.023293	0.010457	0.003402	0.005788	2.227	0.587	26.38
FRC2	0.046445	0.026819	0.000842	0.001330	1.731	0.633	36.55
FRC3	0.045270	0.004494	0.013997	0.001620	10.072	8.640	14.42
FRC4	0.025164	0.001778	0.001530	0.000169	14.153	9.032	36.18

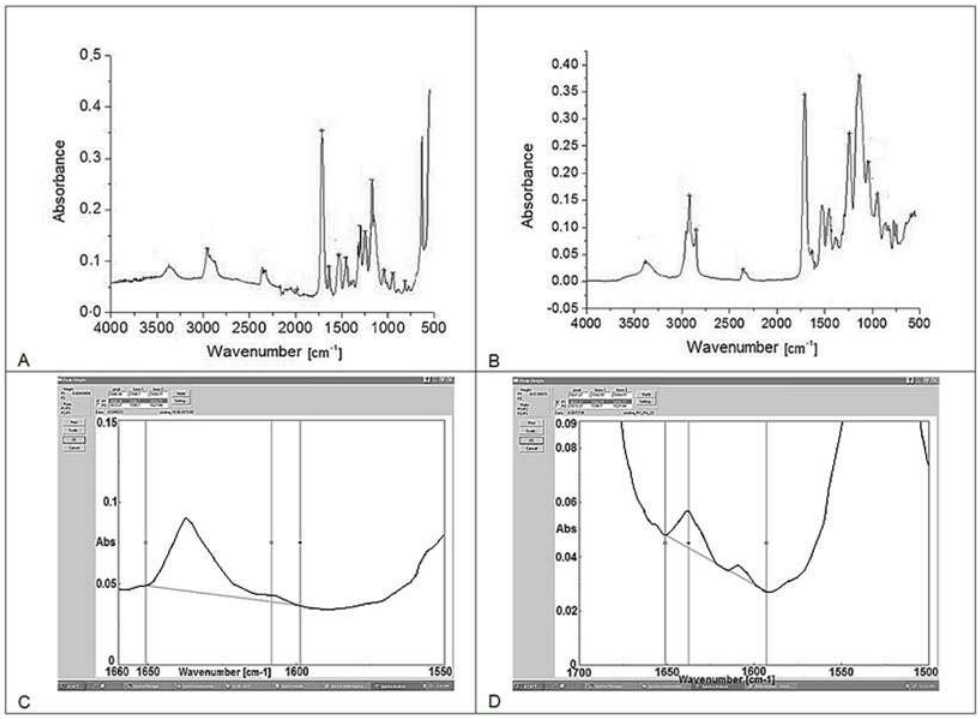

Fig. 1- ATR-FTIR Spectra of R3 resin (before curing) (A) and (C) and of the corresponding C3 copolymer (at 1 days after initiation of polymerization) (B) and (D)/ *Spectrele ATR-FTIR ale răşinii R3 (înainte de polimerizare) (A) şi (C) şi ale copolimerului corespunzător C3 (la o zi de la iniţierea polimerizării) (B) şi (D)* .

The results presented in Table 2 point out that there is a significant difference between the DC recorded in the case of copolymers which contain the Bis-GMA$_{1,2}$/TEGDMA monomers and the copolymers based on the UDMA/TEGDMA monomers. UDMA characterized by a lower viscosity than Bis-GMA$_{1,2}$ and consequently by a longer gel time led to the obtaining of much higher degree of vinyl conversions of the corresponding copolymers. In **T**able 3 is presented the calculation of the RDB for all copolymers. As examples, in figure 1 are presented the FTIR spectra of R3 resin and C3 copolymer at 1 day after polymerization.

3.2. Residual monomer

The percents of Bis-GMA$_{1,2}$, UDMA, TEGDMA si HEMA extracted monomers, related to the weight of initial copolymer sample, and related to the weight of the initial corresponding monomer in the copolymer, respectively, are shown in Table 4 and Figure 2, respectively.

Table 4

Residual monomer extracted from the experimental copolymers related to the initial weight of the copolymer samples
Monomerul rezidual extras din copolimerii experimentali raportat la masa iniţială a probelor de copolimeri

Copolymer	Extracted Bis-GMA %	Extracted TEGDMA %	Extracted UDMA %	Extracted HEMA %
C1	0.008	0.094	-	-
C2	0.054	-	-	0.050
C3	0.001	0.008	0.031	-
C4	0.032	-	0.307	0.110

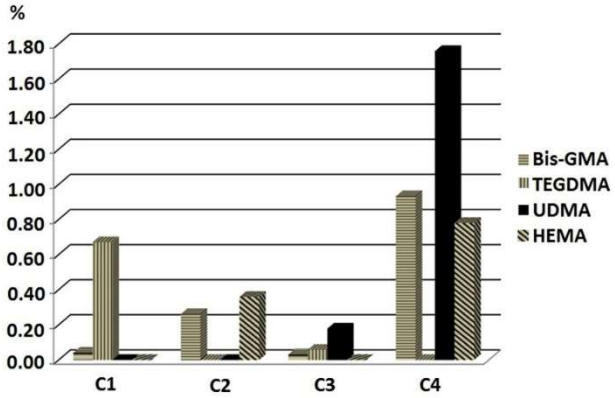

Fig. 2- Residual monomer extracted from the experimental copolymers (related to the of the corresponding initial monomer in the copolimer)/ *Monomerul rezidual extras din copolimerii experimentali (raportat la masa de monomer introdusă în copolimerul corespondent).*

After the polymerization of the dymethacrylic monomers, it is desirable that the amount of residual monomer to be as small as possible, as the unreacted monomer is extracted in time, from the material, having a potential impact not only on the structural stability of the FRC implant, but also on the biocompatibility of the material.

The data presented in table 4 outlines the fact that the monomer extracted from all the elaborated copolymers does not exceed a total value of 0.5% of extracted monomers, in relation to the initial weight of the copolymer sample (0.102% in the case of C1; 0.104% in the case of C2; 0.04% in the case of C3; 0.449% in the case

of C4). These results are smaller than the data presented in the literature for the dental composites, which end up releasing, after 7 days of storing in ethyl alcohol, up to 6% of their components [29] and up to 1.2% residual monomer [30].

As noted above, the smallest quantity of residual monomer is extracted in the case of copolymer C3, while the largest one is associated with the case of copolymer C4. Of these, within the same sample, UDMA and HEMA represent the largest quantity that is extracted, followed by monomer TEGDMA, with the smallest one being the mixture of oligomers Bis-GMA$_{1.2}$ (Figure 2). This behavior can be explained due to the hydrophilic character, as well as the size and flexibility of the each monomer's specific molecules, but also by the degree of crosslinking of each polymeric network. With HEMA and UDMA being hydrophilic, flexible monomers, they can be easily extracted in a hydrophilic medium (water, alcohol). TEGDMA is an aliphatic, less hydrophilic monomer, with relatively flexible etheric groups, whereas the Bis-GMA$_{1.2}$ oligomers have large, rigid molecules, presenting a stronger hydrophobic character compared to the other monomers, which leads to a smaller quantity of extracted monomer. The fact that a significantly smaller quantity of monomer is extracted from C3, in comparison with the other copolymers, highlights the degree of crosslinking of the C3 polymeric matrix as being the highest.

Taking into account the aim of obtaining personalized implants, of particular shapes and sizes, resin R3 was selected for future studies (determining the mechanical properties and the biologic assay).

3.3. Flexural properties

For the determination of the flexural properties, a series of fiber reinforced composites (FRCs) using UDMA-based resin matrix (R3) and continuous unidirectional bundles, respectively woven E-glass fibers (10±1μm diameter) was obtained. The continuous unidirectional bundles were obtained by extracting the continuous bundles from the woven E-glass fibers. The flexural strengths and flexural modulus for the continuous and woven FRCs were determined (table 5).

As one can see from Table 5, the type of fibers has a major influence upon the flexural strength values. The FRCs based on linear bundles of fibers recorded higher values for flexural strength than the FRCs based on woven E-glass fibers. The highest values for flexural strength were obtained in the case of FRC which contained 20 continuous unidirectional bundles of E-glass fibers (717.5 Mpa for flexural strength and 21.7 Gpa for Young's modulus). The FRCs based on woven E-glass fibers having similar reinforcement presented twice smaller values for flexural strengths and 1.5 times smaller values for Young's modulus than FRC based on the unidirectional E-glass fibers.

3.4. SEM analysis

Surface morphology of the samples is shown in Figure 3. The E glass fibers are well incorporated into the polymer matrix and no monofilaments could be seen on the surface. The quality of the surface is good and the roughness is acceptable for a bone implant.

The fracture appearances of the experimental FRCs as the consequence of the flexural stress are shown in Figure 4.

In Figure 4a, one can clearly observe the propagation direction of the crack in the polymer matrix of the cFRC2. The image reveals many broken fibers, but also fibers that bridge the ends of the broken matrix. When force is applied, the matrix is the first to break, while the fibers act as crack stoppers, by transferring the stress from the matrix to the fibers [31]. In Figures 4b and 4c one can see details of the crack presented in Figure 4a.

The SEM images presented in Figures 4d, 4e and 4f show the distribution of the glass fibers in cFRC1 after the removal of the polymer matrix. The presence of the polymer can be observed on the fibers' surfaces. The interaction of the polymer matrix with a single fiber is highlighted in Figure 4g where the fiber is covered with a layer of polymer of irregular shape, which demonstrates a good adhesion between the polymer matrix and the fibers in the case of cFRC1.

The EDX analysis (Figure 4n) shows the constitutive elements of the sample presented in Figure 4g. They are silicon, calcium, aluminum, magnesium, sodium, potassium and oxygen found in the E-glass fiber and carbon that is found in the

Table 5

The flexural properties of the investigated FRCs/ *Rezistenţele la încovoiere ale FRC investigate*

Code FRC	E-glass fibers	Reinforcement %	Flexural strength (Mpa)	Young's modulus (Gpa)
cFRC1	20 continuous unidirectional bundles	65	717.50	21.706
cFRC2	15 continuous unidirectional bundles	57	546.02	16.707
wFRC1	8 woven E-glass fibres	63	372.45	13.295
wFRC2	6 woven E-glass fibres	60	319.35	14.849

-

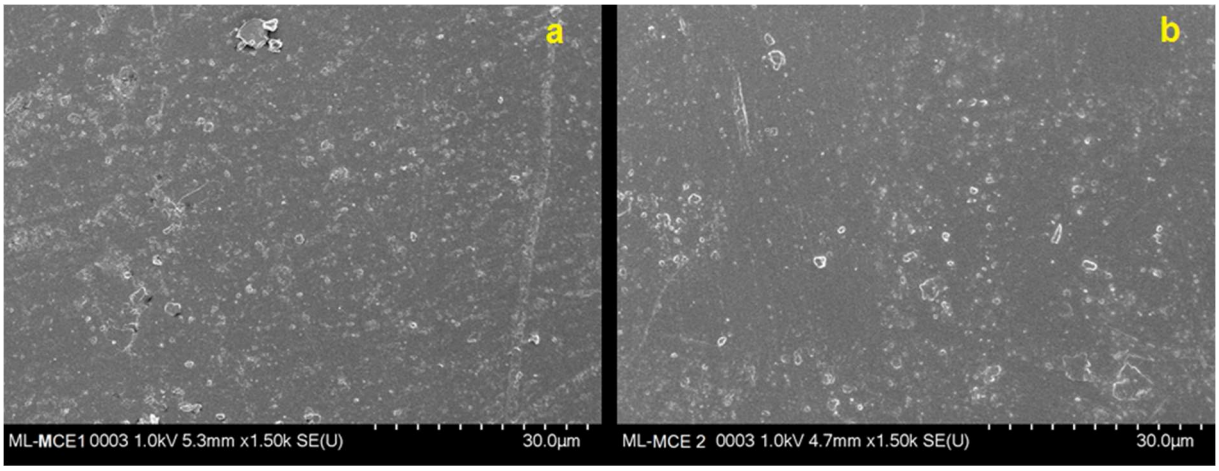

Fig. 3- SEM micrographs of the surface of FRC samples: cFRC1(a) and wFRC1 (b)/ *Imagini SEM ale suprafeţelor epruvetelor de FRC: cFRC1(a) şi wFRC1 (b).*

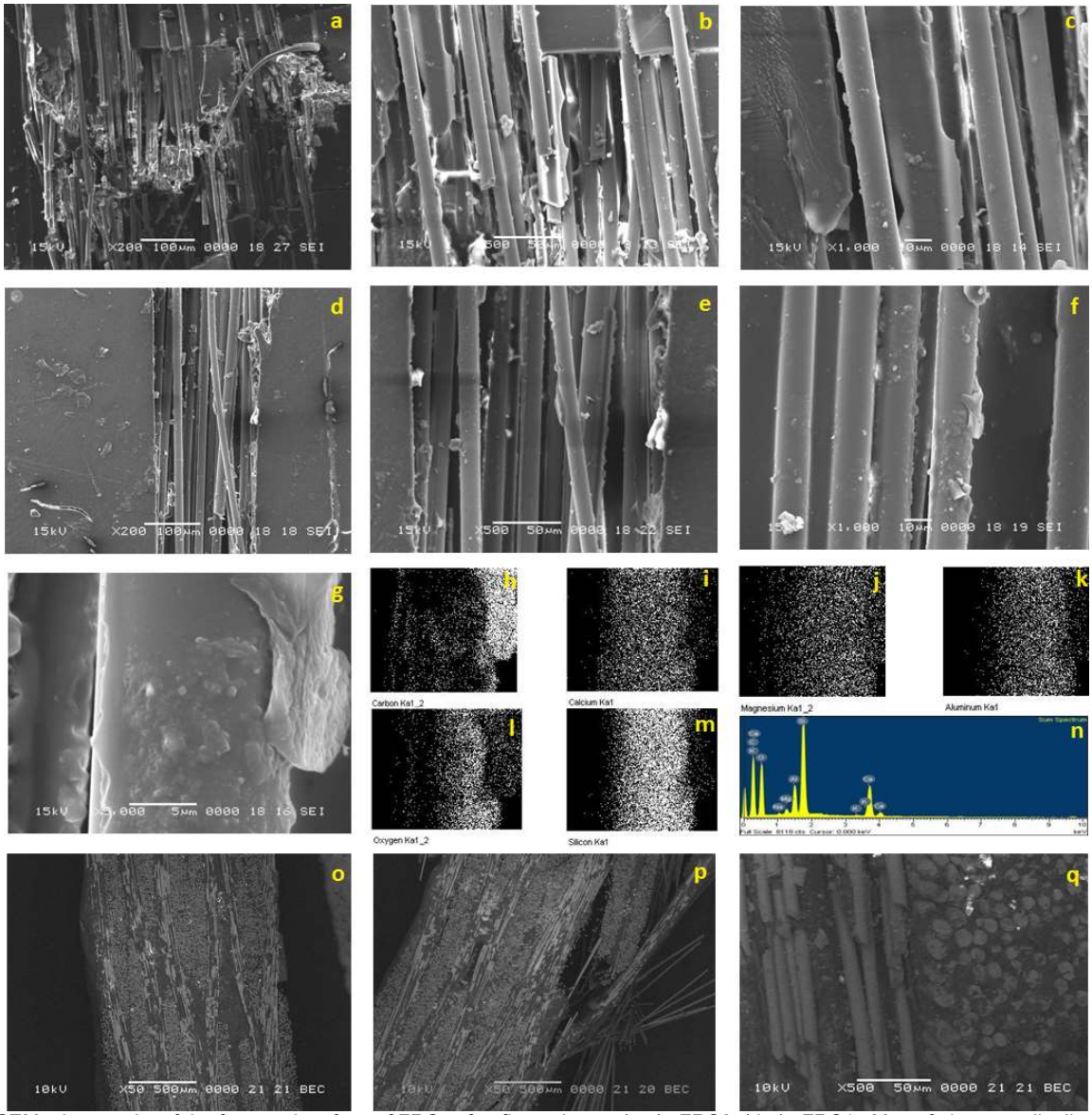

Fig. 4- SEM micrographs of the fractured surface of FRCs after flexural test : (a-c) cFRC2; (d-g) cFRC1; Map of elements distribution for the sample showed in 4g image: (h- carbon, i-calcium, j-magnesium, k-aluminum, l-oxygen, m-silicon); EDX spectrum related to the sample showed in 4g image (n); SEM micrographs of wFRC1 before (o) and after the flexural test (p, q)/ *Imagini SEM ale suprafeţelor fracturate ale FRC după testul de încovoiere: (a-c) cFRC2; (d-g) cFRC1; Harta distribuţiei elementelor pentru proba din imaginea 4g: (h-carbon, i-calciu, j-magneziu, k-aluminiu, l-oxigen, m-siliciu); Spectrul EDX al probei din imaginea 4g (n); Imaginile SEM ale wFRC1 înainte (o) şi după testul de încovoiere (p, q).*

polymer matrix, respectively. The distribution of the main elements in the investigated sample surface is presented in Figures 4h-4m.

All the elements have a relative uniform distribution. The relative uniform distribution of the carbon on the sample surface (Figure 4h) confirms the aforesaid.

The Figure 4o presents the initial state and the Figures 4p and 4q present the fractured appearance of the wFRC1. As one can see only a cracking (breaking) of the outer fibers of the sample appears, the central area suffers only a plastic stretch in the longitudinal direction of the fibers.

3.5. Biological assay

The local biological response to the implanted FRCs depends not only on the chemical properties of the materials, but also on the response to the associated trauma of surgery. Proper surgical technique, adequate preparation of the samples and good quality of their surface ensure a valid result for the implantation test.

After the implantation, no changes in general status and behavior were noticed. Healing of the skin wound at the implant site occurred without any complications. Implants were well tolerated with a very short convalescence time, clinically insignificant, without rejection signs.

Macroscopically, there was no difference between the two groups. Neither necrosis, nor hemorrhage was noticed. Generally, histopathological examination revealed that the muscle tissue reaction to the implants consisted in: moderate fibrosis, mild chronic inflammation and minimal amount of fatty infiltrate (Figure 5). The fibrous capsule (arrows in Figure 5) at the interface between the material and the muscle tissue was well developed and completely surrounded the implant (* in Figure 5).

Several adipose infiltrates were present on the outer surface of the capsule. On the implant trajectory, the muscle was replaced by connective tissue and accessory implants could be identified as smaller material fragments (arrow heads in Figure 5).

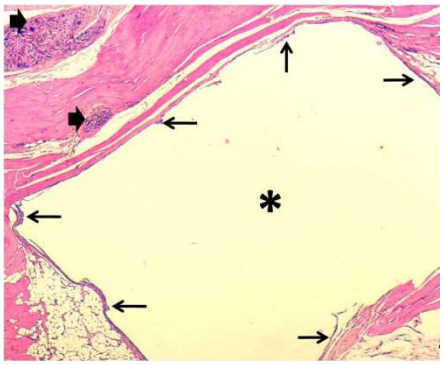

Fig. 5 - Rat muscle tissue reaction to the implant made of cFRC, hematoxylin and eosin stain, 40x/ *Reacţia ţesutului muscular la implantarea epruvetelor din cFRC, coloraţie hematoxilină-eozină, 40x*

The capsule consisted of collagen fibers that were densely packed into bundles and organised on several layers; numerous fibroblasts were associated with the fibers. In the proximity of the implants, a mild chronic inflammatory reaction, including macrophages and lymphocytes, was present. Several capillaries and adipose cells organised into clusters could be seen next to the capsule. Regenerating muscle cells could be seen in the tissue next to the implant, demonstrating the tendency of the muscle to restore to the normal structure (Figure 6).

Table 6

Scores of inflammation for FRC samples in muscle implantation test, according to ISO 10993-6: 2007/ *Scorurile de inflamaţie atribuite epruvetelor confecţionate din materiale compozite pentru testul de implantare intramusculară, calculate după ISO 10993-6: 2007*

	cFRC1 samples										**wFRC1 samples**									
Histological aspect	s 1	s 2	s 3	s 4	s 5	s 6	s 7	s 8	s 9	s 10	s 1	s 2	s 3	s 4	s 5	s 6	s 7	s 8	s 9	s 10
polymorphonuclear cells	0	0	0	0	0	0	0	0	0	0	0	0	0	0	0	0	0	0	0	0
lymphocytes	2	1	1	1	1	1	1	1	1	1	2	1	1	1	1	1	1	1	0	1
plasma cells	0	0	0	0	0	0	0	0	0	0	0	0	0	0	0	0	0	0	0	0
macrophages	1	1	1	1	1	0	0	0	1	1	1	1	1	1	1	1	1	1	1	1
giant cells	0	0	0	0	0	0	0	0	0	0	0	0	0	0	0	0	0	0	0	0
necrosis	0	0	0	0	0	0	0	0	0	0	0	0	0	0	0	0	0	0	0	0
sub-total x 2	6	4	4	4	4	2	2	2	2	2	6	4	4	4	4	4	4	4	2	4
neovascularisation	1	1	1	1	2	1	2	1	1	1	1	1	1	1	1	1	1	1	1	1
fibrosis	1	1	1	1	1	1	1	1	2	1	1	1	1	1	1	1	2	1	2	1
fatty infiltrate	0	1	1	1	1	1	1	2	1	1	0	1	1	2	1	1	1	2	1	1
sub-total	2	3	3	3	4	3	4	4	4	3	2	3	3	4	3	3	4	4	4	3
total	8	7	7	7	8	5	6	6	6	5	8	7	7	8	7	7	8	8	6	7
mean	**6.5**										**7.3**									
stdev	**1.080123**										**0.674949**									

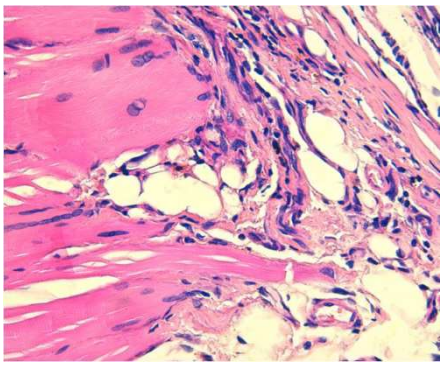

Fig. 6- The fibrous capsule surrounding the implant; muscle cells adjacent to the implant showed tendency to regenerate. hematoxylin and eosin stain, 400x/ *Capsula conjunctivă care înconjoară implantul; celulele musculare adiacente implantului prezintă tendinţă de regenerare, coloraţie hematoxilină-eozină, 400x*

For both of the FRCs, scores attributed to each specimen, according to the intensity of the inflammatory reaction were analyzed and results are presented in Table 6.

Taking into account the aspects observed, the score of inflammation was 6.5±1.080 for cFRC and 7.3±0.674 for wFRC. According to ISO 10993-6 recommendations, the FRCs tested were considered slight irritant (average score between 3.0 and 8.9) and no significant difference between the groups could be assessed. The fiber-glass type (continuous unidirectional bundles of fiber glass or woven fiber glass) doesn't interfere with the biological behavior of FRCs in a significant manner ($p \geq 0.05$).

4. Conclusion

A series of four experimental resins based on Bis-GMA$_{1,2}$ oligomers, UDMA, TEGDMA and HEMA were prepared. The conversion of the resins was evaluated by determining the residual double bonds and the residual monomer presented in the copolymer matrix after 1 day from the initiation of the polymerization.

Based on the conversion results, a series of fiber-reinforced composites were obtained by reinforcing the resin that contained UDMA/Bis-GMA$_{1,2}$/TEGDMA monomer mixture with unidirectional and woven E-glass fibers, respectively.

The flexural strengths for the FRCs were determined and the fracture appearance was investigated by SEM analysis. Biological behavior was assessed by muscle implantation test. Intramuscular inoculation was well tolerated by all subjects, which indicates that E-glass fibers reinforced composites are suitable for medical use purpose.

The results pointed out that the FRCs based on urethane dimethacrylate resin reinforced with woven E-glass fibers could be good candidates for the reconstruction of large cranial bone defects.

Acknowledgements

The research was partially supported by Romanian Executive Unit for Financing Education Higher, Research Development and Innovation, code PN-II-PT-PCCA 2013-4-0917, grant no 115/2014.

REFERENCES

1. S. Aydin, B. Kucukyuruk, B. Abuzayed, and G. Z. Sanus, Cranioplasty: review of materials and techniques, Journal of neurosciences in rural practice 2011, **2**(2), 162.
2. U. Spetzger, V. Vougioukas, and J. Schipper, Materials and techniques for osseous skull reconstruction, Minimally Invasive Therapy & Allied Technologies 2010, **19**(2), 110-121.
3. M. E. Elsalanty, and D. G. Genecov, Bone grafts in craniofacial surgery, Craniomaxillofacial trauma & reconstruction 2009, **2**(3), 125.
4. C. E. Raposo-Amaral, D. F. Bueno, A. B. Almeida, V. Jorgetti, C. C. Costa, C. H. Gouveia, and N. Alonso, Is bone transplantation the gold standard for repair of alveolar bone defects?, Journal of tissue engineering **2014,** 5, doi: 10.1177/2041731413519352
5. N. N. Hung, Basic Knowledge of Bone Grafting. INTECH Open Access Publisher 2012, p 11-33.
6. R. L. Reis, and D. Cohn (Eds.). (). Polymer based systems on tissue engineering, replacement and regeneration (Vol. 86), Springer Science & Business Media 2012.
7. B. L. Eppley, M. Kilgo, J. J. Coleman 3rd, Cranial reconstruction with computer-generated hard-tissue replacement patient-matched implants: indications, surgical technique, and long-term follow-up, Plastic and reconstructive surgery 2002, **109**(3), 864-871.
8. J. Parthasarathy, 3D modeling, custom implants and its future perspectives in craniofacial surgery, Annals of maxillofacial surgery 2014, **4**(1), 9.
9. P. Bártolo, and B. Bidanda, Bio-materials and prototyping applications in medicine, New York, NY, USA: Springer 2008, p 79-107.
10. A. L. Jardini, M. A. Larosa, R. Maciel Filho, C. A. de Carvalho Zavaglia, L. F. Bernardes, C. S. Lambert, and P. Kharmandayan, Cranial reconstruction: 3D biomodel and custom-built implant created using additive manufacturing, Journal of Cranio-Maxillofacial Surgery 2014, **42**(8), 1877-1884.
11. M. J. Peltola, P. K. Vallittu, V. Vuorinen, A. A. Aho, A. Puntala, and K. M. Aitasalo, Novel composite implant in craniofacial bone reconstruction. European Archives of Oto-Rhino-Laryngology 2012, **269**(2), 623-628.
12. K. Alvarez, and H. Nakajima, Metallic scaffolds for bone regeneration, Materials 2009, **2**(3), 790-832.
13. A. Neumann, and K.Kevenhoerster, Biomaterials for craniofacial reconstruction. GMS current topics in otorhinolaryngology, head and neck surgery 2009, **88**, S48-63.
14. M. Özcan, and C. Hämmerle, Titanium as a reconstruction and implant material in dentistry: Advantages and pitfalls, Materials 2012, **5**(9), 1528-1545.
15. J. E. Zins, C. J. Langevin, and S. Nasir, Controversies in skull reconstruction, Journal of Craniofacial Surgery 2010, **21**(6), 1755-1760.
16. J. E. Zins, A.Moreira-Gonzalez, and F. A. Papay, Use of calcium-based bone cements in the repair of large, full-thickness cranial defects: a caution. Plastic and reconstructive surgery 2007, **120**(5), 1332-1342.
17. S. K. Nandi, B. Kundu, and S. Datta, Development and Applications of Varieties of Bioactive Glass Compositions in Dental Surgery, Third Generation Tissue Engineering, Orthopaedic Surgery and as Drug Delivery System, INTECH Open Access Publisher 2011.
18. J. R. Jones, Review of bioactive glass: from Hench to hybrids, Acta biomaterialia 2013, **9**(1), 4457-4486.
19. E. Neovius, and T. Engstrand, Craniofacial reconstruction with bone and biomaterials: Review over the last 11 years, Journal of plastic, reconstructive & aesthetic surgery 2010, **63**(10), 1615-1623.

20. S. M. Kurtz, and J. N. Devine, PEEK biomaterials in trauma, orthopedic, and spinal implants. Biomaterials 2007, **28**(32), 4845.
21. S. M. Kurtz, PEEK biomaterials handbook. William Andrew 2011, p 256.
22. C. Prejmerean, M. Moldovan, L. Silaghi-Dumitrescu, D. Prodan, G. Furtos, M. Trif, and R. Silaghi-Dumitrescu, Composition Versus Physico-mechanical Properties of Some Dental Experimental Polymers, Materiale Plastice 2011, **48**(1), 27.
23. M. Sonmez, D. Ficai, A. Ficai, L. Alexandrescu, G. Voicu, and E. Andronescu, Functionalization of glass fibers for obtaining polypropylene based composite materials, *Revista Romana de Materiale-Romanian Journal of Materials* 2014, **44**(1), 88.
24. M. Sönmez, M. Georgescu, M. Vâlsan, M. Rădulescu, D. Ficai, G. Voicu, and L. Alexandrescu, Design and characterization of polypropylene matrix/glass fibers composite materials, Journal of Applied Polymer Science 2015, **132**(26)
25. G. Furtos, B. Baldea, and L. Silaghi-Dumitrescu, Development of new radiopaque glass fiber posts, Materials science and engineering 2016, **59**, 855.
26. I. Ruyter, and P. P. Györösi, An infrared spectroscopic study of sealants, European Journal of Oral Sciences 1976, **84**(6), 396.
27. ISO 10993-6:2007, Biological evaluation of medical devices- Part 6: Tests for local effects after implantation
28. A. Peutzfeldt, Resin composites in dentistry: the monomer systems, European journal of oral sciences 1997, **105**(2), 97.
29. M. Anne Rathbun, R. G. Craig, C. T. Hanks, and F. E. Filisko, Cytotoxicity of a BIS-GMA dental composite before and after leaching in organic solvents, Journal of biomedical materials research 1991, **25**(4), 443.
30. K. Inoue, and I. Hayashi, Residual monomer (Bis-GMA) of composite resins, Journal of Oral Rehabilitation 1982, **9**(6), 493.
31. G. Furtos, L. Silaghi-Dumitrescu, M. Moldovan, B. Baldea, R. Trusca, and C. Prejmerean, Influence of filler/reinforcing agent and post-curing on the flexural properties of woven and unidirectional glass fiber-reinforced composites, Journal of Materials Science 2012, **47**(7), 3305.

****

MANIFESTĂRI ȘTIINȚIFICE / SCIENTIFIC EVENTS

MAY 31 – JUNE 3, 2016

ISBBB 2016 Sustainable Bioeconomy to Marketplace

14th International Symposium on Bioplastics, Biocomposites and Biorefining

Guelph · Canada

This symposium was created to reflect the broadening scope of ongoing research activities and new developments in the areas of biobased polymers and biorefinery, which have been added as key focus areas. This important international meeting will also continue to examine the ongoing innovations in the fields of biocomposites and green composites, and include a special focus on sustainability and durability of biobased materials for broad applications.

ISBBB 2016 will include oral and poster presentations in addition to industrial exhibits, and will feature plenary speakers and keynote talks by world-leading experts in all focus areas. The conference setting will also allow numerous networking opportunities, and encourage discussions and knowledge transfer of policy aspects and sustainability of biobased products.

http://isbbb.org/Contact

****